

Thermal conductivity of deformed carbon nanotubes

Wei-Rong Zhong¹, Mao-Ping Zhang¹, Dong-Qin Zheng¹, and Bao-Quan Ai^{2*}

¹*Department of Physics and Siyuan Laboratory, College of Science and Engineering,*

Jinan University, Guangzhou 510632, P. R. China and

²*Laboratory of Quantum Information Technology, ICMP and SPTE,*

South China Normal University, Guangzhou, 510006 P. R. China

(Dated: May 26, 2018)

Abstract

We investigate the thermal conductivity of four types of deformed carbon nanotubes by using the nonequilibrium molecular dynamics method. It is reported that various deformations have different influence on the thermal properties of carbon nanotubes. For the bending carbon nanotubes, the thermal conductivity is independent on the bending angle. However, the thermal conductivity increases lightly with XY-distortion and decreases rapidly with Z-distortion. The thermal conductivity does not change with the screw ratio before the breaking of carbon nanotubes but decreases sharply after the critical screw ratio.

Due to lots of potential applications of carbon nanotubes (CNTs), more and more attentions have been given to the exceptional and unique electronic and thermal properties of CNTs in the past few years^{1,2,3,4}. Berber et al⁵ applied molecular dynamics (MD) simulations to study the thermal conductivity of CNTs. They found that CNTs show an unusually high thermal conductivity value of 6600W/mK at room temperature. Pop et al⁶ represented an experimental estimate that the thermal conductance is approximately 2.4 nW/K, and the thermal conductivity is nearly 3500 W/mK at room temperature for a SWNT of length 2.6 μm and diameter 1.7 nm. The result of MD calculation is about two times that of experimental estimate.

Generally, the differences between experiment and theory can be explained by two aspects. Firstly, the thermal characteristics extracted in experiment must rely on an assessment of the SWNT temperature, which is very difficult to obtain experimentally in a quantitative manner^{7,8}. Secondly, CNTs used in MD simulations are perfect structures, however, perfect CNTs are hardly to obtain through experiment. The former will depend on the improvement of the experimental conditions. The later, however, should be attributed to the theoretical reasons.

On the other hand, as have been shown by many simulations and experiments, perfect carbon nanotubes (CNTs) perform very good thermal conductivity. However, due to the need of application, it is inevitable that the CNTs would be bended, twisted, stretched and compressed when they are used. Recently, a few studies have reported that imperfect structures, such as defects, deformations and impurities, can affect the thermal conductivity of nanotube significantly^{9,10,11,12,13}. However, no investigations address on the quantitative relationship between the imperfect parameter and the thermal conductivity of CNTs.

In this work we first study the thermal conductivity of four types of deformed carbon nanotubes by using the nonequilibrium molecular dynamics method. Four typical parameters, i.e., the bending angle θ , the screw ratio β/Z_0 , the stretch factor Z'/Z_0 and ellipse ratio e , are defined to describe the deformed degrees of CNTs. By calculating the thermal conductivity of CNTs in various deformed parameters, we try to get the relationship between the thermal conductivity and the deformed parameters, which will be of significance to understand the role of the deformation in the thermal properties of CNTs.

Figure 1 depicts four typical deformed carbon nanotubes. Fig.1(a) shows a normal carbon nanotube. In our simulations, the nanotubes are deformed from two types (zigzag (7,0) and armchair (7,7)) carbon nanotubes with the normal length $Z_0=18$ nm. Fig.1(b) illustrates a bending carbon nanotube with a bending angle θ , here θ is the intersection angle between the normal direction of the two end sections of the tube. If twisting the nanotube around the Z-axial direction,

one can obtain a twisted nanotube. As shown in Fig.1(c), the screw distortion is denoted to the ratio of the twisted angle (β) to the length of the nanotube (Z_0). Z-distortion is the tension and compression along Z-axial direction. As shown in Fig.1(d), the stretch factor is Z'/Z_0 , where Z' and Z_0 are respectively the length of the distortion nanotube and the normal nanotube. Normally, the width of X-axial direction of the carbon nanotube equals to that of Y-axial direction. When applying a force on X- or Y-direction, the nanotube will become a XY-distortion nanotube. As illustrated in Fig.1(e), for XY-distortion nanotube, the ellipse ratio¹⁴, also called the eccentricity of an ellipse, usually denoted by e , is the ratio of the distance between the two foci, to the length of the one axis or $e = 2f/2a = f/a = f/Y$.

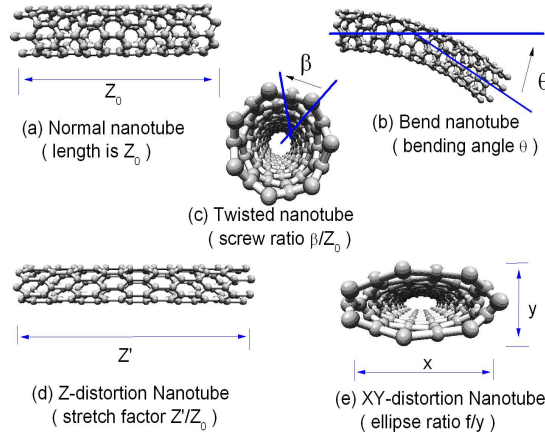


FIG. 1: Normal and four types of deformed carbon nanotubes.

In our simulations, we have used classical molecular dynamics method based on the Tersoff-Brenner potential¹⁵ of C-C bonding interactions. The equations of motion for atoms in either the left or right Nosé-Hoover thermostat are^{16,17,18}

$$\frac{d}{dt}p_i = F_i - \gamma p_i; \frac{d}{dt}\gamma = \frac{1}{Q} \left[\sum_i \frac{p_i^2}{2m_i} - 3Nk_B T_0/2 \right], \quad (1)$$

where p_i is the momentum and F_i is the force applied on the i -th atom. $Q = 3Nk_B T_0 \tau^2/2$, where τ is the relaxation time, which is kept as 1ps. γ is the dynamic parameter of the thermostat, $T(t)$, which is defined as $\frac{m_i}{3k_B}(vx(t)^2 + vy(t)^2 + vz(t)^2)$, where $v(t)$ is the time-dependent velocity, is the instant temperature of the heat baths at time t . T_0 (T_H or T_C), the set temperature of the heat baths, are placed at the two ends of a carbon nanotube and the temperature difference is denoted as $\Delta T = T_H - T_C$. For the convenience of comparison, here we set $T_H = 330K, T_L = 290K$, which are near the room-temperature. In order to keep the shape of the deformed nanotube in the

simulations, we use fixed boundary conditions in the two ends of the nanotube. The fixed region and the heat baths occupy four layers and eight layers of atoms, respectively. N is the number of the atoms in the heat baths, k_B is the Boltzmann constant and m is the mass of the carbon atom.

These equations of motion are integrated by Verlet method¹⁹. The time step is 0.50 fs , and the simulation runs for 2×10^7 time steps giving a total molecular dynamics time of 10 ns . Generally, $T(t)$ can stabilize around the set value T_0 after 1 ns . Time averaging of the temperature and heat current is performed from 5 to 10 ns . The heat bath acts on the particle with a force $-\gamma p_i$; thus the power of heat bath is $-\gamma p_i^2/m$, which can also be regarded as the heat flux from heat bath. The total heat flux injected from the heat bath to the system can be obtained by¹⁸

$$J = \sum_i [-\gamma p_i^2/m_i] = -3\gamma N k_B T(t), \quad (2)$$

where the subscript i runs over all the particles in the thermostat. The final thermal conduction is calculated from the well-known Fourier's law $\kappa = Jl/(\Delta T ch)$, in which l , c , and h ($=0.34 \text{ nm}$) are the length, perimeter and thickness of the carbon nanotubes, respectively.

In order to investigate the chirality dependence of the thermal conductivity, (7,0) and (7,7) deformed CNTs are studied simultaneously in our simulations. There are 1197, 2072 atoms, respectively in the (7,0) and (7,7) CNTs. The deformed parameters of the CNTs include the bending angle, the screw ratio, the stretch factor and the ellipse ratio.

First, we calculate the thermal conductivity of the bending zigzag and armchair CNTs. Figure 2 shows that the thermal conductivity alters slightly with the bending angle not only for zigzag tubes but also for armchair tubes. At the ranges of bending angle from 2 to 50 degrees, the values of thermal conductivity change respectively from 1689 to 1734 W/mK for zigzag CNTs, and from 2263 to 2400 W/mK for armchair CNTs. The fluctuation respectively ranges less than 2.6% and 5.7% . The result shows that the thermal conductivity is independent on the bending angle in the range of error.

We have also investigated the twisted CNTs and found that the screw ratio has no significant influence on the thermal conductivity at the small range of its value. As shown in Fig. 3, for armchair tubes, the thermal conductivity does not change with the screw ratio within the critical value $\beta/Z_0 = 3.0 \text{ deg/nm}$. For zigzag tubes, the critical value is about 15.0 deg/nm . Different behaviors between the zigzag and armchair graphene (or nanotubes) have also been studied by the use of classical as well as quantum molecular dynamics method^{20,21}. In these studies, it is suggested that the critical loading of the zigzag graphene is larger than that of the armchair graphene. Our result exactly, at the view of thermal transport, confirmed that the zigzag CNTs

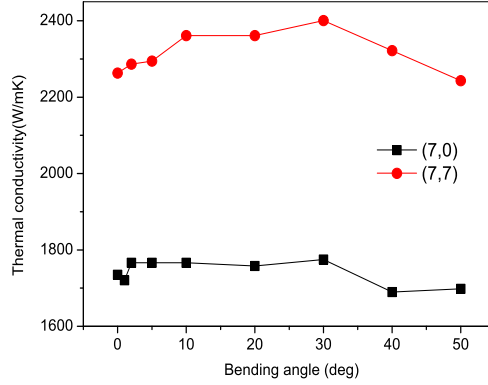


FIG. 2: Thermal conductivity of (7,0) and (7,7) bending carbon nanotubes.

have better mechanical properties than the armchair CNTs. Two states of the zigzag CNTs, state (a) and state (b) in Fig. 3, which are the states before and after breaking respectively, are plotted in Figs. 4(a) and (b). These states correspond to the shapes of CNTs after 10 ns simulations. Similar three states of armchair CNTs in Fig. 3 (points (c), (d) and (e)) are shown in Figs. 4(c), (d) and (e) respectively.

Generally, when the CNTs is twisted (before break off), the chirality of tubes changes and then the atom chains are not parallel to the axis, instead they are in a helix. The vibration of the atoms in deformed nanotubes is apt to have a long path, which causes the low thermal conductivity of deformed nanotubes^{22,13,11}. On the other hand, the ballistic transport is the mainly thermal transport mode for the CNTs at this temperature and length^{23,24}. Since the length of CNTs is invariable when being twisted, the thermal conductivity keeps on a certain value just before the CNTs' break off.

When the screw ratio goes over the critical value, the tubes are breaking, as shown in Figs. 4(b), (d) and (e), an junction occurs in the middle of the tubes, which will increases the resistance of the thermal transport greatly, and then the thermal conductivity drops rapidly.

The thermal conductivity of the Z-distortion as well as the XY-distortion CNTs are also studied. Figure 4 illustrates that not only the tension but also the compression can decreases the thermal conductivity of CNTs strongly. When the stretch ratio $Z'/Z_0 = 0.9$, the thermal conductivity decreases to 45% and 56% of the normal value for armchair and zigzag CNTs, respectively. This phenomenon can be explained to negative influence of the stretching on the full optimization of CNTs. For XY-distortion CNTs, as displayed in Fig.5, the thermal conductivity increases slightly

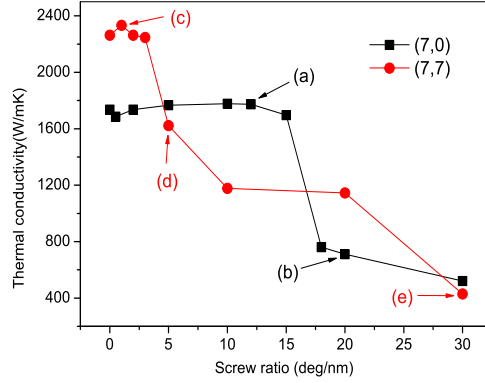


FIG. 3: Thermal conductivity of (7,0) and (7,7) twisted carbon nanotubes. The structures of the CNTs correspond to the points (a), (b), (c), (d) and (e) are displayed in Figs.4(a), (b), (c), (d) and (e) respectively.

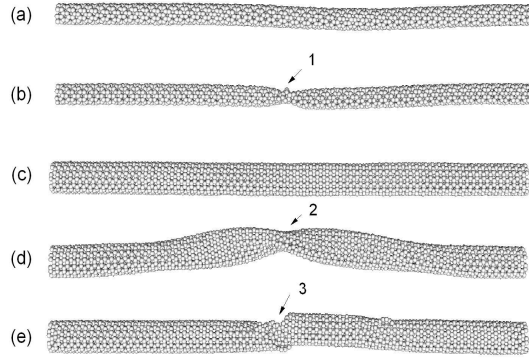


FIG. 4: The shape of CNTs after 5×10^7 steps of simulations. (7,0) CNTs: screw ratio = 12 (a) and 20 (b) deg/nm , position 1 is the breaking junction. (7,7) CNTs: screw ratio = 2.0 (c), 5.0 (d) and 30 (e) deg/nm , position 2 and 3 are the breaking junctions.

when the ellipse ratio is lower or larger than 1. The section area increases as the shape of the CNTs changes from circle to ellipse, which helps the improvement of the thermal conductivity.

Here we have to point out that all deformed parameters set in our calculations are small enough to guarantee against the occurrence of CNTs' snap. For large deformed CNTs, the CNTs will go to a mechanical critical state, and then it is difficult to describe the deformed degrees of CNTs accurately. On the other hand, the temperature we use in the paper is the temperature (T_{MD}) calculated from the classical MD, which can be corrected by taking into account the quantum effects

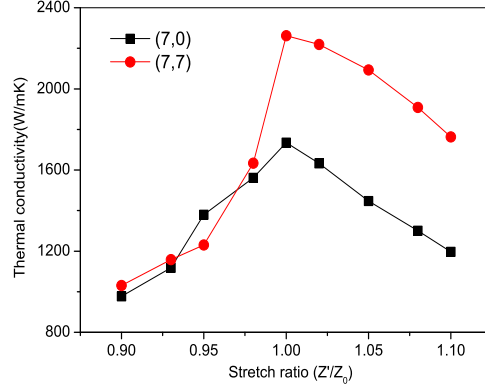


FIG. 5: Thermal conductivity of (7,0) and (7,7) Z-distortion carbon nanotubes.

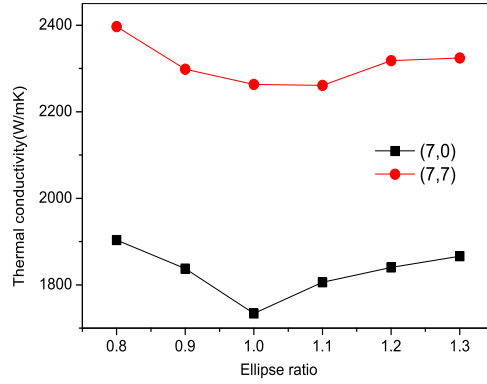


FIG. 6: Thermal conductivity of (7,0) and (7,7) XY-distortion carbon nanotubes.

of phonon occupation, using the expression $T_{MD} = (2T^3/T_D^2) \int_0^{T_D/T} [x^2/(e^x - 1)] dx$, where T and T_D (322 K) are the corrected temperature and Debye temperature, respectively¹⁷.

In summary, we have studied the thermal conductivities of four typical deformed CNTs, using the nonequilibrium MD method based on the Tersoff-Brenner potential. We observed the deformation dependence of the thermal conductivity of CNTs. The thermal conductivity of the bending CNTs does not change with the bending angle. Before the breaking of CNTs, the thermal conductivity is independent on the screw ratio. When the twisting goes over the mechanical criticality, the thermal conductivity decreases rapidly. From the thermal properties of the twisted CNTs, it is suggested that zigzag CNTs maybe have better mechanical property than armchair CNTs. For the distortion in longitudinal and transverse direction, the thermal conductivity increases lightly

with XY-distortion and decreases rapidly with Z-distortion.

Acknowledgments

We would like to thank Siyuan cluster for running part of our programs. This work was supported in part by the National Natural Science Foundation of China (Grant No.11004082) and the Natural Science Foundation of Guangdong Province, China (Grant No.01005249).

* Electronic address: wrzhong@hotmail.com, aibq@scnu.edu.cn

- ¹ E. Pop, Nano Research **3**, 147 (2010).
- ² R. H. Baughman, A.A. Zakhidov, W.A. de Heer, Science **297**, 787 (2002).
- ³ A. Jorio, G. Dresselhaus, Mildred S. Dresselhaus (Eds.), Carbon Nanotubes, Springer Berlin Heidelberg, New York (2008).
- ⁴ X. Li, W. Yang, and B. Liu, Phys. Rev. Lett., **98**, 205502 (2007).
- ⁵ S. Berber, Y. K. Kwon, and D. Tománek, Phys. Rev. Lett., **84**, 4613 (2000).
- ⁶ E. Pop, D. Mann, Q. Wang, K. Goodson, and H. Dai, Nano Lett., **6**, 96-100 (2006).
- ⁷ N. A. Poklonski, E. F. Kislyakov, N. Ngoc Hieu, O.N. Bubel', S. A. Vyrko, A. M. Popov, and Yu. E. Lozovik, Chem. Phys. Lett. **464**, 187–191 (2008).
- ⁸ Y. Xu, G. Ray, and B. Abdel-Magid, Composites: Part A **37**, 114–121 (2006).
- ⁹ C. Tang, W. Guo, and C. Chen, Phys. Rev. B, **79**, 155436 (2009).
- ¹⁰ G. Wu and B. Li, J. Phys.: Condens. Matter, **20**, 175211 (2008).
- ¹¹ J. Lu, J. Wu, W. Duan, and B. Gu, Appl. Phys. Lett. **84**, 4203 (2004).
- ¹² R. Fabian Pease, H. Dai, K. J. Cho, and K. G. Goodson, NSF Nanoscale Science and Engineering Grantees Conference, Dec 16-18, (2003).
- ¹³ W. Zhang, Z. Zhu, F. Wang, T. Wang, L. Sun and Z. Wang, Nanotechnology, **15**, 936–939 (2004).
- ¹⁴ J. W. Harris, and H. Stocker, Handbook of Mathematics and Computational Science. New York: Springer-Verlag, p. 93, (1998).
- ¹⁵ D. W. Brenner, Phys. Rev. B **42**, 9458 (1990); D. W. Brenner, O. A. Shenderova, J. A. Harrison, S. J. Stuart, B. Ni, and S. B. Sinnott, J. Phys.: Condens. Matter **14**, 783 (2002).
- ¹⁶ S. Nosé, J. Chem. Phys. **81**, 511 (1984); W. G. Hoover, Phys. Rev. A **31**, 1695 (1985).
- ¹⁷ J. Hu, X. Ruan, and Y. P. Chen, Nano Lett., **9**, 2730-2735 (2009).
- ¹⁸ G. Wu and B. Li, Phys. Rev. B **76**, 085424 (2007).
- ¹⁹ H. Rafii-Tabar, Computational Physics of Carbon Nanotubes, Cambridge University Press, New York (2008).
- ²⁰ H. Shen, Comp. Mat. Sci. **47**, 220–224 (2009).

- ²¹ Y. Gao, P. Hao, *Physica E*, **41**, 1561–1566 (2009).
- ²² C. Ren, Z. Xu, W. Zhang, Y. Li, Z. Zhu, and P. Huai, *Phys. Lett. A* **374**, 1860–1865 (2010).
- ²³ N. Mingo and D. A. Broido, *Phys. Rev. Lett.* **95**, 096105 (2005).
- ²⁴ J. Wang and J. S. Wang, *Appl. Phys. Lett.* **88**, 111909 (2006).